Parallel Optical Delay Detector for Angle-of-arrival Measurement of a Microwave Signal with Accuracy Monitoring

Z. Cao, H.P.A. van den Boom, E. Tangdiongga, and A.M.J.Koonen

COBRA Institute, Eindhoven University of Technology, NL 5600 MB Eindhoven, The Netherlands
z.cao@tue.nl

A novel parallel optical delay detector for angle-of-arrival measurement is proposed and the measurement errors are experimentally studied and analyzed. Moreover, the measurement accuracy monitoring is investigated.

I Introduction

Determining location of a microwave signal is of great importance for retrieving the position of objects. The parameter angle-of-arrival (AOA) or equivalently the time difference of arrival (TDOA) is required to accurately identify the position. An optical approach to measure AOA can offer many benefits due to its intrinsic features like ultra-low loss and huge bandwidth, which allows high accuracy, and immunity to electromagnetic interference. Moreover, with the rapid development of ultra-low drive voltage electro-optical modulators (EOMs) [1] and high speed photo-diodes [2], barriers between electrical domain and optical domain are gradually eliminated. Recently some photonic approaches are proposed to measure AOAs of microwave signals [3-5]. In Ref.[5], a scheme with two electro-optical modulators (EOMs) and one optical delay line is proposed for AOA measurement. It is in principle an optical delay detector for microwave signals with serial configuration. In this paper, a novel parallel configuration optical delay detector (PODD) with accuracy monitored is proposed based on a dual parallel Mach-Zehnder modulator (P-MZM). Using one P-MZM, the parallel structure can reduce the perturbations. Moreover, the DC-drift induced measurement accuracy degradation can be monitored.
Thereafter, on the same page, follows the paper. The paper should consist of 4 pages. Please do not number the pages. The section headings should be 14 point Times (New) Roman Bold and the body text 12 point Times (New) Roman. Lettering in tables and figures should be 10 point Times (New) Roman. In order to conserve space, references should be given in 10 point. It is recommended that references conform to the IEEE conventions as shown in the example below.

II Operation Principle

The principle of AOA (or TDOA) measurement is schematically depicted in Fig.1. The distance between two antennas (Ante-1 and Ante-2) is denoted as *d*. The AOA is denoted as ψ and the corresponding TDOA can be expressed by $\tau=d\times\cos(\psi)/c$, where c is the light velocity in air. MZ-a and MZ-b are the sub-MZMs inside P-MZM, MZ-c is the tunable phase shift combining MZ-a and MZ-b. The electrical paths (including connections and necessary components like amplifiers) between Ante-1 and MZ-a, Ante-2 and MZ-b will introduce phase differences for different frequencies. Such phase difference can be easily compensated using a look-up table. The delay τ will introduce the phase shift φ between Ante-1 and Ante-2 with the expression $\varphi=\tau\times2\pi f_{mw}$, where f_{mw} is the frequency of the microwave signal. Therefore the task of proposed PODD scheme is to measure the phase shift φ in optical domain. The PODD includes a CW laser, a P-MZM, an optical notch filter, and two power meters. MZ-a and MZ-b are connected to Ante-1 and Ante-2 and the phase shift φ caused by spatial delay τ will be translated to the phase difference of optical sidebands. The following task is to measure the phase difference of optical sidebands by using optical power meters. Both MZ-a and MZ-b are biased to suppress the optical carrier while MZ-c is biased at the maximum point to fully combine optical power from MZ-a and MZ-b. The lightwave from the CW laser is modulated by two replicas of microwave signal at MZ-a and MZ-b with spectrum shown in Fig.1 (a) and (b), respectively. The output optical signals from both MZ-a and MZ-b with phase shift φ are then combined at MZ-c without any additional phase shift. We assumed that the optical carriers are well rejected. The total output power is related to the phase shift φ with expression $P=(E_0J_{+1}(m))^2(1+\cos(\varphi))$, where E_0 is the amplitude of the optical carrier. $J_{+1}(m)$ is the Bessel function of first kind with regard to modulation index (m). It indicates that amplitudes of sidebands relate to the modulation index. The high order sidebands are negligible for low driving power, which is the case of AOA measurement. The value required for AOA estimation is the normalized power, thus the value of E_0 and $J_{+1}(m)$ are less relevant. We can obtain the expression for AOA and TODA as:

$$\varphi = \arccos(P_n - 1), \tau = \arccos(P_n - 1)(2\pi f_{mw})^{-1}, \psi = \arccos\left(\tau c / d\right), P_n = P_m / P_0 \qquad (1)$$

According to Eq.1, to get the values of τ and ψ, the required parameters are P_n and f_{mw}. The P_n can be obtained by measuring P_m and P_0. P_0 is measured with zero phase shift but P_m is measured with unknown phase shift. If f_{mw} is unknown, an additional photonic scheme can be utilized to perform frequency measurement before AOA measurement. Thus the measurement of AOA (or TODA) is then translated into measurement of P_m. In the above discussion, we assume that the optical carriers are well suppressed, and thus the power and phase shift can be fully modeled according to Eq.1. However, both limited extinction ratio (LER) and DC-drift will introduce imperfect suppression (IS) of optical carriers. As shown in Fig.1(I), the DC-drift will introduce the phase shift to the optical carrier and thus to the sidebands. The phase shift in optical carrier leads to IS and the phase shift in sidebands will disturb the final measurement results. Both DC-drifts in MZ-a and MZ-b will introduce similar effect. For the IS induced by LER, since no additional phase shift in sidebands is added, it can be removed via an optical notch filter (ONF). Thus it is of interest to monitor the DC-drift during the measurement. Since the DC-drift is related to the IS, the power measurement of optical carrier can be used to monitor DC-drift. As shown in Fig.1, an ONF (ONF-1 shown in Fig.1) is employed to deeply separate the optical carrier and sidebands. The DC-drift during the measurement can be well monitored. Moreover the IS induced by LER can be eliminated after this process.

III Experimental Setup and Results

Fig. 2 shows the proof-of-concept experimental setup of AOA measurement based on PODD. The optical carrier is generated from a DFB laser at 1550.016nm with 1dBm optical output power. It is fed into a P-MZM after a polarization controller (PC). MZ-a and MZ-b are both biased at their minimum points of power transfer curves. Two commercial microwave sources (LO-1 and LO-2) are synchronized and are employed to

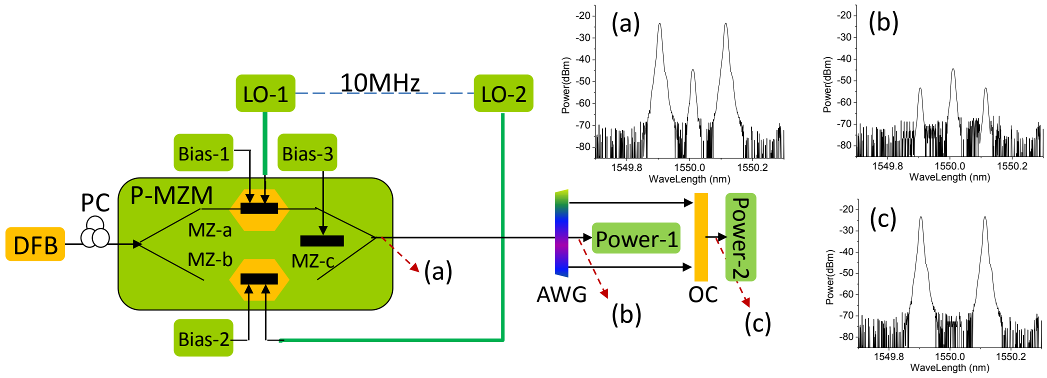

Fig. 2 The experimental setup of AOA measurement based on parallel optical delay detector

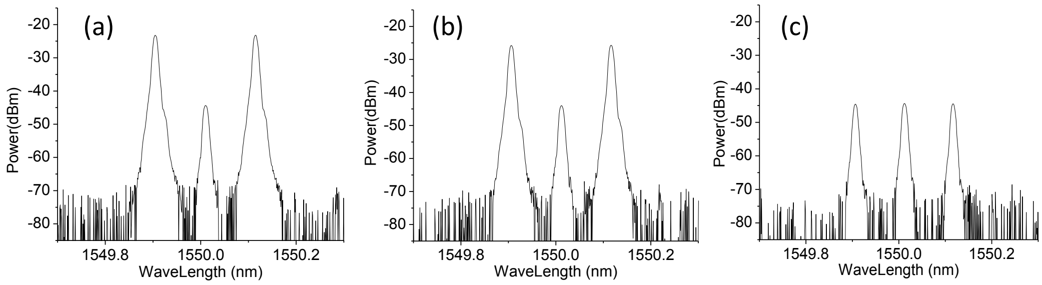

Fig. 3 The measured spectrum for (a) 0° phase shift, (b) 90° phase shift, and (c) 180° phase shift

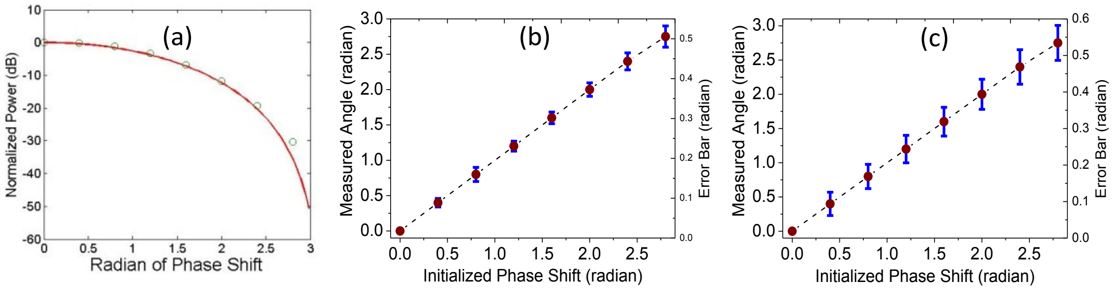

Fig. 4. (a) Measured optical power (circles) and theoretical trend (curve); (b) Measured phase shift (dots) and their measurement errors (vertical bars), P_{mo}=-47.6dBm; (c) Measured phase shift (dots) and their measurement errors (vertical bars), P_{mo}=-41.7dBm;

drive MZ-a and MZ-b at frequency of 12.5GHz. A 10MHz sine signal generated from LO-1 is sent to LO-2 for synchronization. MZ-c is biased at the maximum point of its power transfer curve and the optical spectrum of combined signal is shown in Fig.2 (a). The phase difference between LO-1 and LO-2 induced by different electrical paths is calibrated by a commercial sampling oscilloscope (digital communication analyzer). The output optical signal is then separated by an array waveguide grating (AWG) which acts as an optical notch filter. The channel space of the AWG is 12.5GHz and the signal is then separated into three channels. The optical carrier is in the middle channel (noted as CH-2) and two sidebands are in two neighbor channels (noted as CH-1,3). The signal from CH-2 is used for DC-drift monitoring (measured at Power-1) and its spectrum is shown in Fig.2 (b). Optical signals from CH-1,3 are then coupled again via a 3-dB coupler (OC) for power measurement (at Power-2). Its spectrum is shown in Fig.2 (c). The measured spectrums from CH-1,3 with different phase shifts are shown in Fig.3. We can clearly observe that the power of sidebands degrades when the phase shift increases. In Fig.3 (a) - (c), the optical carrier is not completely suppressed mainly due to LER, because the DC-drift is mostly eliminated by optimizing biases at the initial stage. The power of filtered optical carrier (Pm0) is -47.6dBm at the beginning with biases optimized. And then we measure the phase shift φ and corresponding measurement errors. After a few tens of minutes, the Pm0 increased to -41.7dBm, the measurement errors are evaluated again for comparison. The measured powers versus different phase shifts (circles) are shown in Fig. 4(a). The theoretical power distribution (red curve) versus phase shift is also shown in Fig. 4(a). An accepted agreement is obtained. The measured phase shifts with their measurement errors are shown in Fig. 4(b) and (c). The measurement errors are less than 0.2 radian within the range from 0 to 2.8 (0° to 160°) when the filtered power is -47.6dBm. It is clear that the measurement errors increase when the phase shift goes to π (the measured power decreases). This is partially because of imperfect destruction of sidebands induced by LER. Comparing Fig.4 (b) and (c), it is obvious that the measurement errors increase when Pm0 drifts to -41.7dBm. It shows that the measurement accuracy caused by DC-drift can be well monitored in this scheme. Note that the zero phase shift is used for normalization and thus its measurement error is not applicable.

IV Conclusion

We have proposed a parallel optical delay detector for angle-of-arrival measurement with accuracy monitored. The spatial delay measurement is translated into the phase shift between two replicas of a microwave signal. The phase shifts from 0 radian to 2.8 radian are measured with 0.2 radian measurement error. Moreover, the measurement accuracy monitoring is investigated.

Acknowledge

The authors would like to thank Sesilia Kriswandhi and Arjen Bakker from Phoenix Software (http://www.phoenixbv.com/), and Ronald Broeke from Bright Photonics (http://www.brightphotonics.eu/) for their valuable discussions. This work is supported by The Netherlands Organization for Scientific Research NWO under the project grant Smart Optical-Wireless In-Home Communication Infrastructure (SOWICI).

References

[1] M. Jarrahi, *et al.*, "Wideband, Low Driving Voltage Traveling-Wave Mach–Zehnder Modulator for RF Photonics," *Photonics Technology Letters, IEEE,* vol. 20, pp. 517-519, 2008.

[2] L. Yu-Tai, *et al.*, "Characterization and Comparison of GaAs/AlGaAs Uni-Traveling Carrier and Separated-Transport-Recombination Photodiode Based High-Power Sub-THz Photonic Transmitters," *Quantum Electronics, IEEE Journal of,* vol. 46, pp. 19-27, 2010.

[3] S. Pan, *et al.*, "Photonic approach to the simultaneous measurement of the frequency, amplitude, pulse width, and time of arrival of a microwave signal," *Opt. Lett.,* vol. 37, pp. 7-9, 2012.

[4] X. Zou, *et al.*, "Photonic approach to the measurement of time-difference-of-arrival and angle-of-arrival of a microwave signal," *Opt. Lett.,* vol. 37, pp. 755-757, 2012.

[5] R. K. Mohan, *et al.*, " Frequency resolved angle and time difference of arrival estimation with spatial spectral holography" OFC2010, p.OWF3